This document is the unedited Author's version of a Submitted Work that was subsequently accepted for publication in Angewandte Chemie International Edition English after peer review. The reference of the final edited and published work is Angew. Chem. Int. Ed. 2019, 58, 3501-3505; DOI: 10.1002/anie.201813419

$Rh^{I}Ar/Au^{I}Ar'$ Transmetalation, a Case of Group Exchange Pivoting on Formation of M–M' Bonds *via* Oxidative Insertion

M. N. Peñas-Defrutos,[a] C. Bartolomé,*[a] M. García-Melchor,*[b] and P. Espinet*[a]

Abstract: By combining kinetic experiments, theoretical calculations and microkinetic modelling, we show that the Pf/Rf ($C_6F_5/C_6Cl_2F_3$) exchange between [AuPf($AsPh_3$)] and *trans*-[RhRf(CO)($AsPh_3$)$_2$] does not occur through the typical concerted Pf/Rf transmetalation *via* electron deficient double bridges. Instead, it involves asymmetric oxidative insertion of the Rh^{I} complex into the (Ph_3As)Au–Pf bond producing a [(Ph_3As)Au–RhPfRf(CO)($AsPh_3$)$_2$] intermediate, followed by isomerization and reductive elimination of [AuRf($AsPh_3$)]. Interesting differences are found between the LAu–Ar asymmetric oxidative insertion and the classical oxidative addition process of H_2 to Vaska's complexes.

Bimetallic catalysis [1] generally concerns homogeneous processes in which two transition metals (TM), or one TM and one group-11 element (M), [2] cooperate in a synthetic transformation (often C−C coupling) where their two catalytic cycles are linked by a transmetalation step. [M]–R^1 can be an intermediate previously formed from a main group [MG]–R^1 organometallics in a first cycle, which subsequently acts as a nucleophile towards TM in a second cycle (*e.g.* in gold assisted Stille reactions). In that case three metals (*e.g.* Sn, Au, Pd) are involved. [3] An archetypical transmetalation mechanism is the X/R^1 (X = halide) exchange between [M]–R^1 nucleophiles and [TMR^2]–X electrophiles *via* a cyclic transition state structure with the two metals connected through mixed X/R bridges (eqn. 1). The catalytic processes can suffer complications due to the reversibility of these transmetalations and the existence of undesired secondary transmetalations.[4]

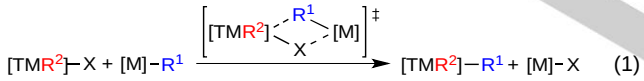

(1)

Transmetalation reactions not only are important in cross-coupling processes. In fact, they can operate whenever [M]–X or [M]–R compounds of different (or identical) metals coexist in solution. Surprisingly, despite their ubiquitous presence and important consequences therefrom, these exchanges are often overlooked. For this reason, their mechanisms are poorly understood. Concerning Rh, we recently reported that the Pf/Rf transmetalation between [$Rh^{III}Cp^*Pf_2$] (Pf = C_6F_5) and [$Rh^{III}Cp^*Rf_2$] (Rf = $C_6F_3Cl_2$-3,5) takes place only when triggered by the catalytic presence of [$Rh^{III}Cp^*Ar(OH)$] (Ar = Pf, Rf), which allows for the formation of mixed Ar/OH bridges in the exchange mechanism.[5] We also discovered a dramatic mechanistic switch in the Ar/X exchange between $Sn^{IV}Ph(^nBu)_3$ and [$Au^{I}XL$] complexes: the typical concerted mechanism involving Ar/X mixed bridges operates when X = Cl, whereas an oxidative addition/reductive elimination (OA/RE) pathway *via* a formally Au^{II}–Sn^{III} intermediate takes over when X = vinyl. [6] A similar OA/RE mechanism involving Au^{I}–Pd^{II} intermediates had been earlier proposed (based on kinetic studies) for the [AuArL] catalyzed *cis*- to *trans*-[$PdAr_2L_2$] isomerization, the first homogeneous Au catalysis ever reported.[7]

In the present work, we investigate the reversible Rf/Pf aryl exchange between linear [AuPf($AsPh_3$)] (**1**) and square-planar *trans*-[RhRf(CO)($AsPh_3$)$_2$] (**2**) to yield [AuRf($AsPh_3$)] (**3**) and *trans*-[RhPf(CO)($AsPh_3$)$_2$] (**4**) (eqn. 2; Xray structures of **1**, **2**, and **4** are given in SI). Kinetic and density functional theory (DFT) calculations uncover an unexpected mechanism operating in this apparently simple system.

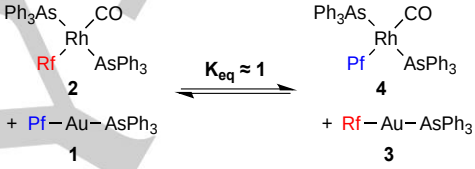

(2)

The highly preferred *trans* disposition of the carbonyl ligand relative to Ar in the Rh^{I} metal centre guarantees that formation of other isomers will not complicate the study. The exchange reaction (1:1 molar ratio) in dry THF as solvent reached the equilibrium in *ca.* 24 hours at 294 K, leading to similar concentrations of the four species ($K_{eq} \approx 1$). This means that the bond energy difference [(M−C_{Pf}) – (M−C_{Rf})] for M = Rh is very similar to the difference for M = Au, hence resulting in a very small ΔG_0 for the overall equilibrium. The reaction was ^{19}F NMR monitored, in the region where the F_{ortho} signals of Pf and the F_{para} of the Rf appear (Figure 1). Neither by-products nor reaction intermediates were detected.

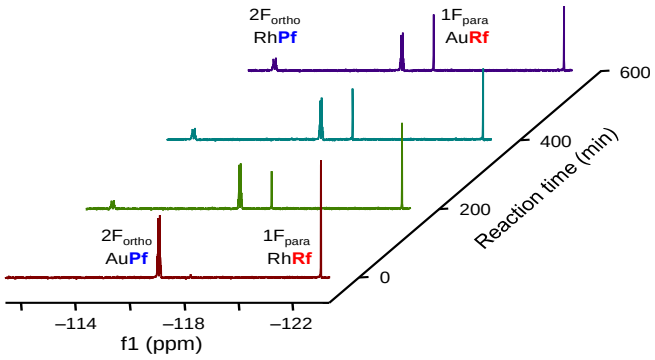

Figure 1. Reaction between [AuPf($AsPh_3$)] (**1**) and *trans*-[RhRf(CO)($AsPh_3$)$_2$] (**2**) in THF at 294 K, monitored by ^{19}F NMR until 40% conversion.

When measuring reaction kinetics, one should be aware that equilibria are chemical reactions where the starting reagents are

[a] Mr. Marconi N. Peñas-Defrutos, Dr. Camino Bartolomé, and Prof. Dr. Pablo Espinet.
IU CINQUIMA/Química Inorgánica, Facultad de Ciencias, Universidad de Valladolid, 47071-Valladolid (Spain).
E-mails: caminob@qi.uva.es and espinet@qi.uva.es
[b] Dr, Maximiliano García-Melchor
School of Chemistry, Trinity College Dublin, College Green, Dublin 2, Ireland. E-mail: GARCIAMM@tcd.ie

Supporting information for this article is given via a link at the end of the document.

regenerated by the reverse reaction, at increasing rate as the system approaches the equilibrium. Fortunately, working at 284 K the aryl exchange studied here has an appropriate rate for very precise monitoring, and the initial rate method can be applied within margins of negligible influence of the reverse reaction (consumption of reactants **1** and **2** lower than 10%), to obtain an experimental value of the initial rate (r_0).[8] The integrals of well-separated signals, *i.e.* the decreasing F_{ortho} signal of reactant **2** (doublet for F_{ortho}–Rh coupling) and the rising sharp F_{para} signal of product **3**, were monitored. Additional experiments using different Au:Rh ratios confirmed a kinetic reaction order 1 on the concentration of both metal complexes, as expected (details in SI). Least squares adjustment using these data (Figure 2a) yielded a reaction rate $r_0 = 1.08\times10^{-7}$ mol L^{-1} s^{-1}. In a simple process this would correspond to an activation Gibbs energy of $\Delta G^{\ddagger}_{initial}$ = 20.6 kcal mol^{-1} for a single rate determining step. However this is not a correct interpretation for the more complex mechanism operating here, as discussed below. The kinetic effect of added free arsine ligand on the initial reaction rate was then quantified by measuring the decelerating effect upon addition of different percentages of $AsPh_3$ (from 5% to 250%), yielding a ligand dependence $[AsPh_3]^{-0.53}$ (Figure 2b).[9,10]

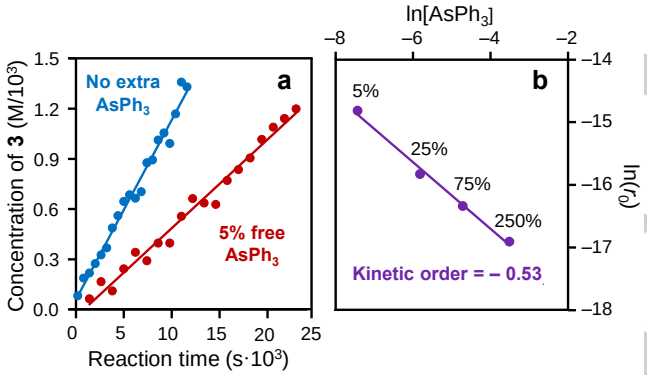

Figure 2. (a) Kinetic plot for the reaction between **1** and **2** in THF at 284K, with (red line) and without (blue line) an excess of free arsine ligand (+ 5% $AsPh_3$). (b) Change in r_0 upon addition of different amounts of free $AsPh_3$ at 298 K.

The high computed DFT Gibbs energies (wb97xd level in THF, at the experimental temperature of 284 K and 1 atm) for $AsPh_3$ dissociation from the starting square-planar Rh^{I} complex **2** (27.1 kcal mol^{-1}) or from the Au^{I} complex **1** (31.5 kcal mol^{-1}) allow us to discard these potentially initial routes as the origin of $[AsPh_3]$ dependence. Moreover, the addition of only 5% $AsPh_3$ ligand already results in a large decrease of the reaction rate by a factor of 0.52 (Figure 2a), suggesting that added $AsPh_3$ is operating on some lower concentration intermediate and not on **1** or **2**. The data point towards a mechanism far from the *rate-determining step* oversimplification, [11] and support that the kinetics observed must depend on more than one transition state.

For a closer examination of the problem, multivariant kinetic analysis using COPASI,[12] and DFT calculations were used (see SI for details). With new data in hand, a reversible reaction path that fits very well all the experimental observations could be proposed (Figure 3). The profile combines: 1) computed transition states and intermediates by means of DFT calculations (blue lines);[13] 2) plausible structures, with COPASI-adjusted energies (red and pink lines). The COPASI adjustment leads to an $AsPh_3$ kinetic dependence $[AsPh_3]^{-0.64}$, very close to the experimental value. Since the energy profile is very symmetric, only the first half is discussed.

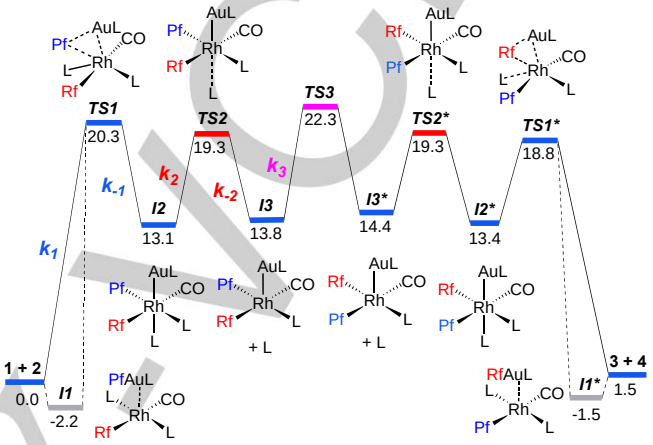

Figure 3. Gibbs energy profile for the transmetalation reaction between **1** and **2,** in THF at 284 K and 1 atm.

Starting from the initial complexes **1** and **2**, the DFT simulations found a van der Waals complex ***I1*** (in grey), which is non-existing in solution in the presence of solvating THF molecules. Otherwise, being ***I1*** hypothetically more stable than **1** and **2**, it should be observed experimentally. Artifacts of this kind may arise in simulations in the absence of explicit solvent molecules and hence, must be discarded (unless experimentally observed) to calculate $\Delta G^{\ddagger}$.

The process starts with the oxidative addition of the Au–Pf bond to Rh, *via* the transition state ***TS1***. This first step requires an energy barrier of 20.3 kcal mol^{-1} and gives rise to the octahedral complex ***I2***, where the Au atom is in the axial position and the Pf moiety is in the equatorial plane, in *cis* position to the Rf group. From ***I2***, calculations indicate that the dissociation of the arsine ligand in the axial position to afford the 5-coordinate intermediate ***I3*** is almost thermoneutral. The corresponding transition state (***TS2***) is barrierless in gas phase (see Figure SI13) and was not found, which is frequent for L dissociations by progressive bond elongation (Figure S13). Estimations of coordination transition states in the literature suggest a reasonable value about 4.5 kcal mol^{-1} higher than ***I3***, due to diffusion cost in solution.[14] The value proposed in the profile, calculated by kinetic COPASI adjustment, is 19.3 kcal mol^{-1}, that is 5.5 kcal mol^{-1} higher than ***I3*** (see details in SI). This is an excellent fitting with the literature expectations. Finally, the process requires isomerization from the 5-coordinate species ***I3*** to ***I3**** before the rest of the process progresses symmetrically. The isomerization of 5-coordinate species has been extensively theoretically studied showing that many reaction pathways are possible with activation energies within 10 kcal mol^{-1}.[15] Using

COPASI, we estimated the energy of the transition state for (***TS3***) to be 8.5 kcal mol^{-1} higher than ***I3*** ($\Delta G^{\ddagger}$ = 22.3 kcal mol^{-1}). It is worth noting that the $AsPh_3$ dissociation barrier for the octahedral complex ***I2***, is considerably lower than calculated for the square-planar precursor. This can be rationalized considering that the *trans-influence* of the different ligands is $LAu^- > Pf^- > AsPh_3$, which is supported by the order of Rh–As bond distances in complexes **2** and ***I2***: (Rh–As$_{trans\ to\ Au}$ = 2.688 Å in ***I2***) > (Rh–As$_{trans\ to\ Pf}$ = 2.520 Å in **I2**) > (Rh–As$_{trans\ to\ As}$ = 2.421 Å in **2**). Thus, the M–M bond strongly facilitates the dissociation of the ligand in trans.

The large effect on the reaction rate of a small amount of added $AsPh_3$ is now easily understood observing that the arsine operates on the dissociative step from ***I2*** to ***I3*** *via* ***TS2***: the 5% of arsine relative to the initial concentration of complexes **1** and **2** is, in fact, an enormous excess relative to the concentrations of **I2** or **I3** in equilibrium.[16] Indeed, the correct interpretation of the $AsPh_3$/**2** ≈ 0.05 concentration ratio (corresponding in fact to $AsPh_3$/***I2*** ≈ 10^{11} at the correct reaction point) indicates that added $AsPh_3$ is very inefficient at preventing its dissociation from ***I2***. In other words, $AsPh_3$ trans to Au($AsPh_3$) behaves as a very weak ligand (which is consistent with the close energies of ***I2*** and ***I3***), and also as fairly labile ($\Delta G^{\ddagger}$ = 5.5 kcal mol^{-1} from ***I2***).

The combined DFT plus experimental energy profile in Figure 3 illustrates how the $RfRh^{I}$/$PfAu^{I}$ exchange occurs through different coordination geometries (square-planar, octahedral and square pyramidal), different oxidation states for the Rh and Au centers, and an isomerization process *via* 5-coordinate intermediates. Geometrical details of the evolution from the initial square-planar Rh^{I} complex **2** (including ***I1*** for comparison) are summarized in Figure 4. It clearly shows a parallel approximation of the Pf–AuL bond over the **L–Rh–L** axis, which induces progressive closure of the L–Rh–L angle and concomitant elongation of the Pf–AuL bond in ***TS1***. This eventually results in the *cis*-addition of the Pf and AuL groups to complex **2**, giving rise to the octahedral complex ***I2***. At this point the high trans influence of the AuL group facilitates dissociation of the $AsPh_3$ ligand in trans, giving the 5-coordinate ***I3*** from which isomerization occurs. The formation of the two other possible octahedral isomers arising from approximation of the Pf–AuL bond along the **Rf–Rh–CO** direction (two possible orientations) was also considered, but were discarded based on their high computed activation energies (more than 10 kcal mol^{-1} higher than ***TS1***, see SI for details).

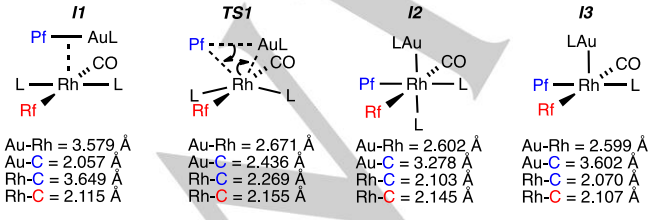

Figure 1. Evolution of bond distances along the reaction pathway. **Sum of covalent radii**: Au-Rh = 2.78 Å; Au-C = 2.09 Å; Rh-C = 2.15 Å.

This NBO analysis indicates that the Rh–Au bond in **TS1** involves the electron donation of a filled *4d* orbital from Rh^{I} into an empty 6s orbital of Au, and the back-donation of a filled *5d* orbital from Au into an anti-bonding orbital mainly constituted by a hybrid *sd* orbital from Rh (Figure 5a,b). The sum of the two (mostly 5a, see Table S4) contributes to make the Rh–Au bond. The NBO analysis also suggests that Au center does not participate in the formation of the Rh–Pf bond. This interaction is initiated instead by electron donation from a hybrid *sp* orbital of the Pf group to an empty hybrid *sd* orbital from Rh (Figure 5c). In short, our analysis supports that the formation of the Rh–Au bond using electron density from Rh prepares the formation of the Pf–Rh bond by polarizing the electron density of the Au–Pf bond towards the Pf ipso carbon atom. In other words, the *oxidative addition* is the result of an *asymmetric oxidative insertion* of the electron donor Rh: into the Pf–AuL bond.

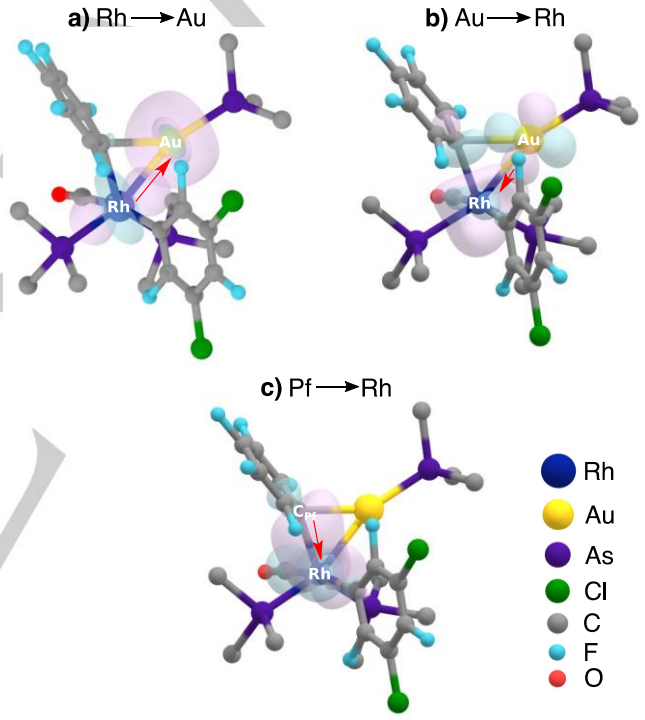

Figure 1. Isosurfaces (isovalue = 0.05 e$^-$ bohr^3) of the NBOs in ***TS1***. *Above*: a)+b) electron-donation from Rh and Au to make the Rh–Au bond; it can alternatively be defined as Rh-to-Au donation + Au-to-Rh back-donation. *Below*: c) electron donation from the Pf^- group making the C–Rh bond, while breaking the C–Au bond. H atoms are omitted and $AsPh_3$ is drawn as AsC_3 for better observation.

The geometrical evolution discussed above, in which two ligands in *trans* (CO and Rf) remain as mere spectators, is reminiscent of the classical oxidative addition of H_2 to the Vaska's type complex *trans*-[MCl(CO)(PPh_3)$_2$] (M = Rh, Ir).[17] In the latter, however, the L–M–L axis remains passive while the more electron poor Cl–M–CO axis undergoes angle bending;[18] the process involves electron donation of the electron pair of the H–H bond to Rh,[19] eventually leading to a different isomer when back-donation from Rh cleaves the H–H bond.[20]

Some concepts used in the text deserve some comment. We are using the uncommon expression *asymmetric oxidative insertion* of Rh into the Au–C bond to define the intimate oxidation/reduction mechanism of the process, at variance with the *symmetric oxidative addition* occurring with H_2 on Vaskas complexes. The rules to assign formal oxidation numbers impose that the M–M' bonds should not count because the electron pair in that bond is supposed to be equally shared between the two metals (non-polarized bond); with this rule, complexes ***I2*** would be assigned Rh^{II} and Au^0 oxidation states, corresponding to an overall one electron oxidation of Rh^I by Au^I. In the latter section we have considered the anionic moiety $[(Ph_3As)Au:]^-$ because classifying ligands in a *trans-influence* list requires to consider them as $2e^-$ donors; within this approach, the complexes would be assigned Rh^{III} and Au^{-I}. Finally, in apparent contradiction, in ***TS1*** the Pf–AuL bond is eventually asymmetrically cleaved providing the Rh center with the fragments LAu^+ and Pf^-. This illustrates how assigning oxidation states may be misleading about the real electron density on the metal, and about bond polarizations. This is better examined by looking at the NPA (natural population analysis) charges on Rh in ***TS1*** and ***I2*** (–1.15 and –1.22 respectively), which show that Rh^{III} has more negative charge than in the Rh^I complex **2** (–0.70). Overall, Rh gains electron density while it is formally being oxidized. The gold atom shows only minor differences between the linear molecule and the octahedral intermediate, with similar slightly positive charges in the range +0.27 to +0.20.

In conclusion, the Rh^IAr/Au^IAr' transmetalation studied here does not follow the traditional Ar/Ar' double-bridged mechanism, but involves an oxidation/reduction mechanism. Moreover this is also an unusual one in that it is initiated by donation of an electron pair from Rh to Au, which eventually triggers the transfer of $[Ar:]^-$ to Rh. Interestingly, the different electronic characteristics of the polar Ar–AuL and the non-polar H–H bonds on Vaska's type complexes induce formation of different octahedral isomers.

Experimental Section

Experimental Details are given in SI.

Acknowledgements

The authors thank the financial support from the Spanish MINECO (projects CTQ2016-80913-P and CTQ2014-52796-P), the Junta de Castilla y León (project VA051P17). The DJEI/DES/SFI/HEA Irish Centre for High-End Computing (ICHEC) is also acknowledged for the provision of computational facilities and support. M. N. P.-D. gratefully acknowledges the Spanish MECD for a FPU scholarship.

Keywords: bimetallic catalysis • Oxidative addition • gold • rhodium • transmetalation mechanism

[1] a) M. H. Pérez-Temprano, J. A. Casares, P. Espinet, *Chem. –Eur. J.*, **2012**, *18*, 1864–1884; b) D. R. Pye, N. P. Mankad, *Chem. Sci.*, **2017**, *8*, 1705–1718.

[2] a) Y. Shi, S. A. Blum, *Organometallics*, **2011**, *30*, 1776–1779; b) J. delPozo, J. A. Casares, P. Espinet, *Chem. – Eur. J.*, **2016**, *22*, 4274–4284; c) R. J. Oeschger, P. Chen, *J. Am. Chem. Soc.*, **2017**, *139*, 1069–1072.

[3] J. delPozo, D. Carrasco, M. H. Pérez-Temprano, M. García-Melchor, R. Álvarez, J. A. Casares, P. Espinet, *Angew. Chem. Int. Ed.*, **2013**, *52,* 2189–2193.

[4] For more details and formation of homocoupling products $R^2–R^2$, see: J. del Pozo, G. Salas, R. Álvarez, J. A. Casares, P. Espinet, *Organometallics*, **2016**, *35*, 3604–3611; and references therein.

[5] M. N. Peñas-Defrutos, C. Bartolomé, M. García-Melchor, P. Espinet, *Chem. Commun.*, **2018**, *54*, 984–987.

[6] D. Carrasco, M. García-Melchor, J. A. Casares, P. Espinet, *Chem. Commun.*, **2016**, *52*, 4305–4308.

[7] A. L. Casado, J. A. Casares, P. Espinet, *Organometallics*, **1997**, *16*, 5730–5736.

[8] The reaction rate when the products formed reaches 10% is proportional to $(0.90)^2 – (0.10)^2 \approx 0.8$. At that point the rate has decreased to 80% of r_0. The rate constant error within this limit, when translated to $\Delta G^{\ddagger}$ values, is < 1 kcal mol^{-1}.

[9] These experiments were carried out at 298 K due to the lower rate in the presence of high concentrations of free arsine.

[10] For a related case of arsine dependence in Pd see: M. H. Pérez-Temprano, J. A. Casares, A. R. de Lera, R. Álvarez, P. Espinet, *Angew. Chem. Int. Ed.*, **2012**, *51*, 4917–4920.

[11] S. Kozuch, S. Shaik, *Acc. Chem. Res.*, **2011**, *44*, 101–110.

[12] S. Hoops, S. Sahle, R. Gauges, C. Lee, J. Pahle, N. Simus, M. Singhal, L. Xu, P. Mendes, U. Kummer, *Bioinformatics*, **2006**, *22*, 3067–3074.

[13] To be more precise (see SI) COPASI produces changes in ***I2*** and ***I3*** (less than 1 kcal mol^{-1}) when the reversibility condition is imposed.

[14] a) C. L. McMullin, J. Jover, J. N. Harvey, N. Fey, *Dalton Trans.,* **2010***, 39,* 10833–10836; b) C. L. McMullin, N. Fey, J. N. Harvey, *Dalton Trans.*, **2014***, 43,* 13545–13556.

[15] R. Asatryan, E. Ruckenstein, J. Hachmann, *Chem. Sci.*, **2017**, *8*, 5512–5525.

[16] For a related case see: C. Bartolomé, Z. Ramiro, M. N. Peñas-Defrutos, P. Espinet, *ACS Catal.*, **2016**, *6*, 6537–6545.

[17] L. Vaska, J. W. DiLuzio, *J. Am. Chem. Soc.*, **1962**, *84*, 679–680.

[18] C. E. Johnson, R. Eisenberg, *J. Am. Chem. Soc.*, **1985**, *107*, 3148–3160.

[19] A. Didieu, A. Strich, *Inorg. Chem.*, **1979**, *18*, 2940–2943.

[20] J. J. Low, W. A. Goddard III, *J. Am. Chem. Soc.*, **1984**, *106*, 6928–6937.